

Manuscript Number:

Title: Recent trends of extreme temperature indices for the Iberian Peninsula

Article Type: SI: EcoHCC14

Keywords: Iberian Peninsula; temperature; extreme events; WRF; climate simulation

Corresponding Author: Ms. Dora Fonseca,

Corresponding Author's Institution:

First Author: Dora Fonseca

Order of Authors: Dora Fonseca; Maria João Carvalho; Martinho Marta-Almeida; Paulo Melo-Gonçalves; Alfredo Rocha

**Abstract:** Climate change and extreme climate events have a significant impact on societies and ecosystems. As a result, climate change projections, especially related with extreme temperature events, has gained increasing importance due to their impacts on the well-being of the population and ecosystems. However, most studies in the field are based on coarse global climate models (GCMs). In this study, we perform a high resolution downscaling simulation to evaluate recent trends of extreme temperature indices. The model used was Weather Research and Forecast (WRF) forced by MPI-ESM-LR, which has been shown to be one of the more robust models to simulate European climate. The domain used in the simulations includes the Iberian Peninsula and the simulation covers the 1986 – 2005 period (i.e. recent past). In order to study extreme temperature events, trends were computed using the Theil-Sen method for a set of temperature indexes defined by the Expert Team on Climate Change Detection and Indices (ETCCDI). For this, daily values of minimum and maximum temperatures were used. The trends of the indexes were computed for annual and seasonal values and the Mann-Kendall Trend test was used to evaluate their statistical significance. In order to validate the results, a second simulation, in which WRF was forced by ERA-Interim, was performed. The results suggest an increase in the number of warm days and warm nights, especially during summer and negative trends for cold nights and cold days for the summer and spring. For the winter, contrary to the expected, the results suggest an increase in cold days and cold nights (warming hiatus). This behavior is supported by the WRF simulation forced by ERA-Interim for the autumn days, pointing to an extension of the warming hiatus phenomenon to the remaining seasons.

Highlights

- Temperature simulation using WRF driven by MPI-ESM-LR and by ERA- Interim
- Trend analysis of the extreme temperature indices over the Iberian Peninsula
- Increase in the annual number of the extreme warm events
- Increase in the cold days and cold nights (both simulations) in winter
- Decrease in the warm nights and days in autumn (ERA-driven)

## Recent trends of extreme temperature indices for the Iberian Peninsula

D. Fonseca<sup>1</sup>, M.J. Carvalho<sup>1</sup>, M. Marta-Almeida<sup>1</sup>, P. Melo-Gonçalves<sup>1</sup>, A. Rocha<sup>1</sup>

<sup>1</sup> CESAM and Dept. Physics, University of Aveiro, Aveiro, Portugal

### ABSTRACT

Climate change and extreme climate events have a significant impact on societies and ecosystems. As a result, climate change projections, especially related with extreme temperature events, has gained increasing importance due to their impacts on the well-being of the population and ecosystems. However, most studies in the field are based on coarse global climate models (GCMs). In this study, we perform a high resolution downscaling simulation to evaluate recent trends of extreme temperature indices. The model used was Weather Research and Forecast (WRF) forced by MPI-ESM-LR, which has been shown to be one of the more robust models to simulate European climate. The domain used in the simulations includes the Iberian Peninsula and the simulation covers the 1986 – 2005 period (i.e. recent past). In order to study extreme temperature events, trends were computed using the Theil-Sen method for a set of temperature indexes defined by the Expert Team on Climate Change Detection and Indices (ETCCDI). For this, daily values of minimum and maximum temperatures were used. The trends of the indexes were computed for annual and seasonal values and the Mann-Kendall Trend test was used to evaluate their statistical significance. In order to validate the results, a second simulation, in which WRF was forced by ERA-Interim, was performed. The results suggest an increase in the number of warm days and warm nights, especially during summer and negative trends for cold nights and cold days for the summer and spring. For the winter, contrary to the expected, the results suggest an increase in cold days and cold nights (warming hiatus). This behavior is supported by the WRF simulation forced by ERA-Interim for the autumn days, pointing to an extension of the warming hiatus phenomenon to the remaining seasons.

**Keywords:** Iberian Peninsula, temperature, extreme events, WRF, climate simulation

### Correspondence

Email: dora.leticia@ua.pt

## 1. Introduction

The Special Report on Extreme Events (SREX) of the Intergovernmental Panel on Climate Change (Field, 2012) mentions evidence that some extremes have changed as a result of anthropogenic influences, including increases in atmospheric concentrations of greenhouse gases. As such, it is probable that anthropogenic influences have led to an increase in extreme minimum and maximum daily temperatures, on a global scale. Extreme temperature events can impact many aspects of human life, such as mortality, health, comfort, agriculture and hydrology (Ciais et al 2005; Garcia-Herrera et al., 2005; Brown et al., 2008; Patz et al., 2005). There is growing evidence that extreme events will become more frequent and more severe in the future (e.g., Kharin and Zwiers, 2000). For this reason, solid projections of changes in the temperature extremes become more important, and have seen an increase in the last decade. In order facilitate the analysis of observed and predicted extremes in, not only temperature, but also in precipitation change, the joint World Meteorological Organization Commission for Climatology (CCI)/World Climate Research Programme (WCRP) project on Climate Variability and Predictability (CLIVAR) Expert Team on Climate Change Detection and Indices (ETCCDI) has defined a set of climate indices (Karl et al.,

1  
2  
3  
4 1999; Peterson et al., 2001). These indices enable a consistent comparison between analyses  
5 performed anywhere in the world and promote the analysis of extremes all over the world,  
6 particularly in less developed countries, by organizing regional climate-change workshops (Zang et  
7 al., 2011).

8  
9 Alexander et al. (2006) noted, that in a great part of the global land there was a significant  
10 decrease in the annual occurrence of cold nights between 1951 and 2003. That is, some regions  
11 might have become less cold, instead of warmer. The study performed by Moberg et al. (2006) over  
12 Europe shows that global conclusions made by Alexander et al. (2006) are not representative of  
13 Europe. They showed a warming both in the daily minimum temperature and the daily maximum  
14 temperature, in agreement with a previous study by Moberg and Jones (2005). In addition, there are  
15 large regional differences in the temperature trend patterns. In a previous study conducted Klein  
16 Tank and Können (2003), a pronounced warming between 1976 and 1999 is mentioned, which is  
17 mainly associated an increase in warm extremes rather than with a decrease in cold extremes. Over  
18 Europe, large scale atmospheric circulation patterns, such as the North Atlantic Oscillation (NAO)  
19 (the most important pattern over Europe), mainly affects the winter temperatures (Efthymiadis et al.,  
20 2011; Espírito Santo et al., 2014). Efthymiadis et al. (2011) refer that cold extremes are associated  
21 with positive NAO phases. In recent studies, a discrepancy between observed and simulated trends in  
22 global mean surface temperature has been observed, leading to more studies on this phenomenon,  
23 such as the ones conducted by Easterling et al. (2009), Meehl et al. (2011) or Sillmann et al. (2014).  
24 These periods are referred to in the literature as hiatus periods (Meehl et al., 2011), and are  
25 characterized by little or no warming trend, and are mostly a winter phenomenon (Kosaka and Xie,  
26 2013). Meehl et al. (2011) indicated the 2000-2009 period as a hiatus period. Recently, Sillmann et al.  
27 (2014) reported that the largest discrepancy between observed and simulated trends in cold extremes  
28 (temperature minimum) is found in the Northern mid-latitudes (20 °N – 45 °N), where observations  
29 indicate a coherent zonal band of decreasing trends between 1996 and 2010. However, Seneviratne  
30 et al. (2014) showed that hot extremes have continued to warm despite the global warming hiatus.

31  
32  
33  
34 Global Climate Models (GCMs) are a fundamental tool for the study of future climate and are  
35 able to capture climate phenomena on a continental or sub-continental scale (Schliep et al. 2010).  
36 They provide data either to estimate large-scale aspects of climate change, to drive regional climate  
37 models or to be used directly by impact models (Barfus, et al. 2014). The fifth phase of the Coupled  
38 Model Intercomparison Project (CMIP5) has made available long-term simulations for the 20th  
39 century climate and projections for the 21st (Taylor, et al. 2012), for which using a set of emission  
40 scenarios, referred to as Representative Concentration Pathways (RCPs) were used (Moss et al.,  
41 2010). This has increased our knowledge of climate variability and climate change. Even though  
42 GCMs, such as those used in CMIP5, provide useful information, such as in the works done by  
43 Sillmann et al. (2013a) and Sillmann et al. (2013b), their low-resolution does not allow for climate  
44 change evaluation at a local scale. Regional Climate Models (RCMs) are used to simulate the space-  
45 time variability of climate change with greater precision than GCMs. Currently, the downscaling  
46 techniques in use nest the RCM within the GCM, allowing simulations over a smaller area with  
47 higher resolution. This comes at the expense of limiting the model domain size, i.e. by focusing over  
48 a limited area. According to Brands et al. (2013), the MPI-ESM-LR model has the best performance  
49 for simulating the temperature over Europe.

50  
51  
52  
53 Several studies have been carried out to explore temperature extremes in the Mediterranean  
54 region (e. g. Kuglitsch et al., 2010) and in Spain (e. g. Esteban-Parra et al., 1995; Cruz and Lage,  
55 2006; Brunet et al., 2007; Del Río et al., 2007; Martínez et al., 2010;). However, although there are  
56 already some studies for the Iberian Peninsula (such as Rodríguez-Puebla et al., 2010;  
57 Fernández-Montes et al., 2012), these studies feature few stations for the Western part of the  
58 Peninsula (Portugal). The same happens with the publicly available data source ECA&D (European  
59  
60  
61  
62  
63  
64  
65

Climate Assessment & Data set website <http://eca.knmi.nl>, Klein Tank et al., 2002) which includes 199 stations for several European countries but with a reduced number of stations over Portugal.

In this paper, we analyse the results of a downscaling simulation to evaluate the high resolution recent trends of extreme temperature indices over the Iberian Peninsula. The WRF simulations forced by ERA-Interim and MPI data, covering the period from 1986 to 2005. Carvalho et al. (2014) compared WRF model results forced with several reanalysis and compared model performance in terms of wind. That study found ERA-Interim as the best WRF driven over Iberian Peninsula.

The paper is organized as follows: Section 2 details the study area, model data basics and the methods applied. The results are presented in Section 3 starting with changes in hot and cold extremes. The conclusions are given in Section 4.

## 2. Data and Methods

### 2.1. Study Area

The region of study is the Iberian Peninsula, located in the southwestern part of Europe (Fig. 1). Its topography is complex with mountains and elevations, more notably the Pyrenees, which connect the Peninsula with France, and reach an altitude of nearly 3400 meters and Sierra Nevada (located in the south of Spain) with of approximately 3500 meters.

The north and west are under influence of the Atlantic Ocean while the south is influenced by the Mediterranean Sea. The rest of the area is coastline, under the influence of the Atlantic Ocean in the North and the West, and the Mediterranean Sea in the South. The region is usually influenced by the cold temperatures of the Atlantic Ocean and the warm temperatures over the Mediterranean Sea and the Sahara desert. The region's particular geography promotes a marked climate gradient from the north to the south, as well as diurnal and seasonal thermal gradients from the coastal areas to the center of the Iberian Peninsula (Dasari et al. 2014). The air temperatures near the surface, especially the cold extremes, are associated with the East Atlantic mode and with the NAO pattern, which is more intense in the Northern Hemisphere (Espírito Santo et al., 2014)).

### 2.2. Regional Simulations

The daily minimum and maximum surface air temperatures used were simulated by the regional model WRF (*Weather Research and Forecasting*) (Skamarock et al., 2008). The initial and boundary conditions used by the RCM were supplied by the (1) MPI-ESM-LR (with the r1i1p1 initialization), which is a GCM with 200 km (1.8750 °) spatial resolution (both in latitude and longitude) and 6-hourly temporal sampling; (2) Era-Interim, with a 0.75° horizontal resolution and the same 6-hourly temporal sampling. This simulation was forced with ERA-Interim to evaluate the performance of the MPI as a driver for WRF. The ERA-Interim is the most recent reanalysis data set provided by the ECMWF and contains selected improvements on the ERA-40, such as representation of the hydrological cycle, the quality of the stratospheric circulation, and the consistency in time of the reanalyzed fields (Dee et al., 2011).

The simulation domains are shown in Fig. 1 with 9 km of spatial resolution, covering the Iberian Peninsula and a portion of the North-Western Atlantic Ocean, with a latitude and longitude ranging from 33° to 45°N and 12°W to 5.5°E, respectively. The temporal domain of simulated data covers the 1986 – 2005 period (i.e. recent past) (see Marta-Almeida et al., 2015).

### 2.3. Methods

In this work, the main goal is to explore the changes in surface temperature extremes, related with extreme cold and hot temperature events. There are several methods to define and characterize extreme temperature events. The approach used in this study to evaluate these changes in extreme temperature events was the annual and seasonal analysis of the trends of the indices of extremes in daily minimum (TN) and maximum (TX) air temperature.

### 2.3.1. Indices

In Table 1, a description of the 17 indices based on the TN and TX is presented, as defined by a team of ETCCDI experts. These indices have been used in several studies about changes in the temperature extremes ([http://etccdi.pacificclimate.org/list\\_27\\_indices.shtml](http://etccdi.pacificclimate.org/list_27_indices.shtml)). The indices can be divided in 4 (Alexander et al., 2006): (1) Percentile, (2) Threshold, (3) Absolute and (4) Duration-based. In general, the percentile-based indices are defined as days over the warmest/coldest long-term percentiles, which include the occurrence of hot days (TX90p), warm nights (TN90p), cold days (TX10p) and cold nights (TN10p). Threshold indices are defined as the number of days in which a maximum or minimum temperature falls above or below a fixed threshold. These include the annual or seasonal occurrence of frost days (FD), ice days (ID), summer days (SU) and tropical nights (TR). Absolute indices represent maximum or minimum values within a season or year. They include maximum daily maximum temperature (TXx), maximum daily minimum temperature (TNx), minimum daily maximum temperature (TXn) and minimum daily minimum temperature (TNn). Duration indices define periods of excessive warmth (WSDI) and coldness (CSDI). There are other indices, such as diurnal temperature range (DTR) and extreme temperature range (ETR) that is computed from TXx and TNn. The reference period considered in this work for the calculation of percentile indices, is the reference period between 1986 and 2005.

Every index is computed for the WRF grid forced by the MPI-ESM-LR (MPI) and Era-interim (ERA) simulations. The analysis performed was restricted to a few indices, after considering the relevance of the entirety of results. The analyzed indices are underlined in Table 1. In the choice of the indices under analysis, previous studies were taken into account, as well as their magnitude of change (i.e. indices with greater expected change were selected). These were computed on an annual and seasonal scale, for the period between 1986 and 2005, that is, one value per year for the period of study. This approach has been used, for instance, by Sillmann et al. (2014). Regarding the seasonal scale, the following periods were considered: spring (March, April and May), summer (June, July and August), autumn (September, October and November) and winter (December, January and February). For the winter of 1986, the December of the previous year is used.

### 2.3.2. Trends estimation

Once the indices for the entire domain have been computed, for both MPI and ERA forced simulations, the seasonal and annual trends were computed using the Theil-Sen method, also known as the ‘‘median of pair-wise slopes’’ nonparametric regression (Theil, 1950 Sen, 1968). Since some of the indices data do not have a Gaussian distribution and, in these cases, a simple linear squares estimation would not be appropriate. Therefore, the statistical significance of the trends was tested using the nonparametric Mann–Kendall test (Wilks, 2011) for 0.05 significance level (p-value < 0.05), against the null hypothesis of no trend. In addition, the spatial means for the minimum and maximum temperature were computed for both simulations, along with their respective trends.

## 3. Results and Discussion

The spatial patterns of the trend for 20 year set of indices were analyzed in order to quantify the variations in temperature extremes, and to verify the presence/absence of a trend for the period between 1986 and 2005 (recent past).

### 3.1. Changes in hot extremes

Recent studies have revealed significant generalized changes in temperature extremes, with a warming trend in every region of the globe (Manton et al., 2001, Peterson et al., 2002, Aguilar et al.,

1  
2  
3  
4 2005, Griffiths et al., 2005 and New et al., 2006). Fig. 2 shows that the 1986-2005 annual trends in  
5 the number of summer days (SU) is positive in the North for MPI-driven simulation and in the South  
6 for ERA-driven simulation (the trend is statistically significant at a 0.05 significance level), with a  
7 maximum of approximately 1 day/year. The differences between these two simulations are higher for  
8 the regions where the trends are higher. The annual trends are mostly due to strong positive trends  
9 simulated for summer (not shown).  
10

11  
12 The annual trend in the number of summer days is also complemented by the TX90p index  
13 (Warm days). Fig. 3 shows the annual trend in warm days for the period between 1986 and 2005. An  
14 increase in the number of warm days of approximately 1 day/year is seen over the North and center  
15 of Portugal for WRF forced by MPI and over the North of Algeria for WRF forced by ERA, where  
16 the trend is statistically significant. The MPI-driven simulation overestimates the number of warm  
17 days over the North and center of Portugal in comparison with the ERA-driven simulation. The  
18 differences between the simulations (MPI-driven and ERA-driven) are under 0.5 days/year, and in  
19 general both simulations points towards an increase in the number of warm days over the Iberian  
20 Peninsula.  
21  
22

23  
24 Looking at the TX90p index (warm days) for winter (Fig. 4), the differences between  
25 simulations increase. In general, the MPI-driven simulation predicts a decrease in the number of  
26 warm days for winter of about 0.3 days/year over the Iberian Peninsula, whereas ERA- driven  
27 simulation indicates an increase in the number of warm days of 0.2 days/year. The differences for  
28 winter trends for the period of 1986 to 2005 between MPI-driven and ERA-driven simulations show  
29 an underestimation of approximately - 0.5 days/year in the number of warm days for simulation MPI  
30 in relation to ERA. For both spring and summer, MPI-driven and ERA-driven are in agreement when  
31 it comes to the sign of the trend over the Iberian Peninsula, with a trend of the number of warm days  
32 of approximately +0.3 days/year. For summer, as in the SU index, the simulation forced by MPI  
33 shows an overestimation in the North/ West of Portugal and an underestimation in the South/ East of  
34 Spain, of about +/-0.3 days/year. These are the regions for which there is a greater difference  
35 between simulations. For the autumn, the MPI-driven shows an increase in the number of warm days  
36 in the North and West of the IP of +0.2 days/year and a trend of -0.2 days/year in the South and East.  
37 The ERA-driven simulation shows a reduction in the number of warm days, which is statistically  
38 significant for most of the domain, with some regions showing a decrease of up to 0.5 days / year.  
39  
40  
41

42 Fig. 5 shows the annual trend of warm nights (TN90p) for the period between 1986 and 2005.  
43 The results for the MPI-driven simulation show a maximum trend over the Iberian Peninsula of +0.8  
44 days/year, i.e. an increase of 0.8 warm nights / year. The regions with highest trends are statistically  
45 significant. The biggest differences between the results obtained for simulation MPI-driven and  
46 ERA-driven are found in the South of the Iberian Peninsula, in which the annual trend of warm  
47 nights is of approximately -0.3 days/year for ERA-driven, and positive for the MPI-driven.  
48  
49

50 For the winter (Fig. 6.), the MPI-driven simulation points towards a -0.2 days/year trend over  
51 Spain, while over Portugal the trend ranges from zero to +0.1 days / year. On the other hand, ERA-  
52 driven has a value of -0.2 days/year in the Southwest of the Iberian Peninsula and of +0.3 days/year  
53 in the North and East. For the summer days, the difference in the number of warm nights for both  
54 simulation. The MPI-driven simulation over the Iberian Peninsula has an increase of 0.3 days/year, a  
55 trend which is statistically significant in the western part of the Iberian Peninsula. For ERA-driven,  
56 there are small regions of increase in the number of warm nights but, in general, and especially in the  
57 West, there is a decrease in warm nights. This trend, however, is not statistically significant. This  
58  
59  
60  
61  
62  
63  
64  
65

1  
2  
3  
4 negative trend in the number of warm nights becomes statistically significant in some regions of  
5 Spain in the autumn, with a value of -0.6 days/year, for the results for the ERA-driven simulation.  
6

7 There is some inconsistency between the simulated trends in warm temperature extreme indices,  
8 especially for the autumn days. The MPI-driven simulation does not represent the cooling observed  
9 in ERA-driven, with a statistically significant trend of -0.5 days and nights / year. However, for  
10 winter, the simulation MPI-driven has a more intense cooling, when compared with ERA-driven. But  
11 in general, taking into account only the spatial pattern of the annual trends between 1986 and 2005,  
12 there is, on average, an increase of + 0.4 days/year of warm days (TX90p) and nights (TN90p).  
13  
14

### 15 **3.2. Changes in cold extremes**

16 A study conducted by Karl et al. (1993) suggests an asymmetric warming of TN and TX, which  
17 is later observed by other studies, especially by Simolo et al. (2011), which proposes a greater  
18 asymmetry in the distribution of TN, for Europe. In this section, cold temperature indices are  
19 analyzed. For the annual trend of FD (Frost Days), Fig. 7, the results obtained for the simulation  
20 MPI-driven show a decrease in the number of frost days over the Pyrenees, with some points in  
21 which the trend is statistically significant. There are also grid points with a positive, statistically  
22 significant trend over regions of higher altitude. On the other hand, the results obtained for the  
23 simulation ERA-driven suggests a decrease in the number of frost days for the center of the Iberian  
24 Peninsula, with a value of approximately -0.5 days/year. However, this trend is not statistically  
25 significant.  
26  
27  
28  
29

30 The annual trend of the number of cold days (TX10p) is shown in Fig. 8. It can be seen that  
31 for the MPI-driven simulation it has positive and negative values of 0.2 days/year, i. e., there are  
32 areas with an increase in the number of cold days, and other areas with a decrease in the number of  
33 cold nights of 0.2 days/year. The difference in the annual trend between simulations is significant in  
34 some areas. The ERA-driven simulation shows a decrease in the number of cold days for the entire  
35 Iberian Peninsula. However, this trend is only statistically significant in the North of Spain.  
36  
37

38 For winter, the MPI-driven simulation (Fig. 9) shows a positive trend of + 0.3 days/year over  
39 the Iberian Peninsula, except for a small region in the East of Spain, which shows a trend of - 0.1  
40 days/year. The differences between the results in the trends obtained for the simulation forced by  
41 MPI and ERA is 0.3 days/year or less, and the results obtained with ERA-driven are, in general,  
42 positive trends. There is an increase in the number of cold days for winter. The difference between  
43 the trends with MPI-driven and ERA-driven simulation for the number of cold days is small, and  
44 both simulation suggest a decrease in the number of cold days for spring. Both simulations have a  
45 trend of -0.4 days/year over the Iberian Peninsula. This negative trend is maintained for summer.  
46 Similarly to the TX90p index (in which the trends in ERA-driven for the autumn show a more  
47 intense decrease in the number of warm days, in comparison with MPI-driven simulation) the ERA  
48 simulations point to a larger increase in the number of cold days, in which the trend over the Center/  
49 South region is of + 0.4 days/year and statistically significant.  
50  
51  
52  
53

54 Fig. 10 shows the annual trend of cold nights (TN10p). For the MPI-driven simulation, the  
55 results show an increase in the number of cold nights over the North of the Iberian Peninsula, and a  
56 decrease over the South. The differences between MPI and ERA are positive in the North and  
57 negative in the South, and of the order of 0.4 days/year.  
58  
59  
60  
61  
62  
63  
64  
65

1  
2  
3  
4 Fig. 11 shows a variation in the pattern of the seasonal trend of the TN10p index (cold  
5 nights). The results for MPI-driven simulation suggest an increase in cold nights over the Iberian  
6 Peninsula, with statistically significant trends in high altitude regions. For spring, both MPI –driven  
7 and ERA-driven simulations show a trend of -0.7 days/year, which are statistically significant in all  
8 domain. The negative trend in the number of cold nights is also observed in the summer, but with a  
9 value of -0.2 for MPI-driven and -0.3 for ERA-driven, in the Southeast of the Iberian Peninsula. The  
10 largest difference between simulations is observed in autumn, with a predominantly negative trend in  
11 TN10p for simulation forced by MPI of -0.1 days/year, and a positive trend in the South/ East of 0.4  
12 days/year for simulation forced by ERA. The difference, therefore, reaches 0.5 days/year.  
13  
14

15  
16 Unlike what happened with warm extremes, in which an annual increase in warm days/nights is  
17 simulated over the Iberian Peninsula, for cold extremes the model does not show a generalized  
18 decrease in the cold days/nights over the Iberian Peninsula. On the contrary, it shows areas where  
19 there is an annual increase in cold days/nights. In addition, there is a greater difference between the  
20 MPI-driven and ERA-driven annual trends than in warm extremes. Several studies have suggested  
21 that the inconsistency between simulated results and observations is explained by a temporary  
22 ‘hiatus’ in global warming, that is referred to as a winter phenomenon (Cohen et al., 2012; Kosaka  
23 and Xie, 2013). In this study, the model shows, not only a cooling in winter, but also in the autumn  
24 months. Furthermore, in ERA-driven simulation, this cooling is more intense for the autumn  
25 (approximately +0.4 cold days/ nights/year) than for the winter (approximately +0.2 cold days/  
26 nights/year). To evaluate if these results depend on the forcing (MPI or ERA) or on the WRF model,  
27 the same indices were calculated for ERA-Interim temperature data for the period between 1986 and  
28 2005. The trends for the indices obtained using this data set (ERA-Interim) also show a more intense  
29 cooling for the autumn months. In recent literature, possible causes for this unexpected finding  
30 between simulated results and observation have already been discussed. The explanations put  
31 forward were: a decrease in stratospheric water vapor (Solomon et al., 2010), an increase in  
32 tropospheric and stratospheric aerosols concentration (Solomon et al 2011, Kaufmann et al. 2011) or  
33 an internal climate variability manifested via La-Niña-like decadal cooling in combination with a  
34 vertical re-distribution of heat in the ocean (Meehl et al 2011; Kosaka and Xie2013; England et al  
35 2014).  
36  
37  
38  
39  
40

### 41 **3.3. The *Hiatus* Period**

42 We computed the average minimum (TN<sub>mean</sub>) and maximum (TX<sub>mean</sub>) time series for the  
43 whole domain, which is shown in Fig. 12. In general, there is a positive trend in the annual mean.  
44 These results are consistent with previous studies based on maximum and minimum temperatures  
45 and their percentiles, which represent an increase in the temperature for the Iberian Peninsula (for  
46 instance, Prieto et al. 2004; Brunet et al., 2007; Martínez et al., 2010 ;Del Rio et al., 2011), with a  
47 maximum value of TX for the MPI model (0.032 degrees/year). In addition, it is seen that the rate of  
48 “observed” warming is slower than the simulated by the model (MPI). This result is observed in  
49 several studies, especially the one carried out by Fyfe et al. (2013), which mentions the  
50 overestimation of global warming over the past 20 years (1993-2012). However, there is no  
51 agreement on the period for which this overestimated global warming occurred, with it varying  
52 between 1996 and 2010 (Silmann et al., 2014) or from 2000 to 2009 (Meehl et al. (2011)).  
53  
54  
55

56 Unlike what happens for the annual means, the seasonal time series for the autumn and winter  
57 show negative trends.

58 Fig. 13a shows the TN and TX time series and their respective trends for the winter days. There  
59 is a negative trend for both the TN and the TX, which indicates a decrease in the minimum and  
60  
61  
62  
63  
64  
65

1  
2  
3  
4 maximum temperature during winter. For TX, the negative trend is due to the last few years, from  
5 1999 to 2005 (warming hiatus). If we were to remove this period, the observed trend would be  
6 positive. Also, the model is able to detect this cooling with very similar trends: MPI with a trend of  
7 -0.023 degrees/year and ERA with -0.024 degrees/year.  
8

9 When it comes to winter days TN, the difference between ERA-driven and MPI-driven  
10 simulation increases, with MPI showing a larger negative trend. Between 1999 and 2005, ERA-  
11 driven simulation of TN shows a decrease in temperature, whereas for MPI-driven the negative trend  
12 is due to the “flattening of the normal distribution”, which means that this negative trend observed in  
13 MPI is not due to a clear decrease in temperature (i. e. the model does not simulate the warming  
14 hiatus). For the autumn days, the time series (Fig. 13b)) shows that MPI-driven has a positive trend,  
15 showing an increase in temperature, whereas ERA-driven has a negative trend. The differences are  
16 more significant for TX than for TN.  
17  
18

#### 19 **4. Conclusions**

20 The goal of this study was to analyze the trends in the extreme temperature indices over the  
21 Iberian Peninsula, using downscaling simulations forced by the MPI-ESM-LR (MPI) and Era-  
22 Interim (ERA), for the period between 1986 and 2005 (recent past). The main conclusions obtained  
23 from this study are the following:  
24  
25

26 - For hot extremes:

27 In general, an increase in the annual number of extreme warm events was detected (summer days  
28 (SU), warm days (TX90p) and warm nights (TN90p)).

29 The annual trends of the warm extreme indices are mostly due to the trend simulated for spring  
30 and summer.  
31

32 The autumn and winter seasonal trends are the ones with the largest difference between simulated  
33 and “observed” (ERA-driven simulations) values which was unexpected for autumn.  
34

35 The ERA-driven simulation has statistically significant negative trends over the Iberian  
36 Peninsula, with warm days (TX90p) and warm nights (TN90p) displaying a decrease of  
37 approximately 1 day/year. For winter, the MPI-driven simulation shows a negative trend for TX90p  
38 that is statistically significant in some regions, which is not the case in the ERA-driven simulations.  
39

40 - For cold extremes:

41 The annual trends obtained for the cold temperature extremes show a greater disparity between  
42 simulated for ERA-Interim and MPI.  
43

44 The results simulated for MPI-driven show regions with positive trends, pointing to an increase  
45 in cold temperature extremes, especially for cold days (TX10p) and cold nights (TN10p).  
46

47 The seasonal trends obtained for spring indicate a decrease in the number of frost days, cold days  
48 and cold nights, with areas where these trends are statistically significant. Especially for cold nights  
49 (TN10p), which have an increase of approximately one day/year.  
50

51 For summer, the negative trends are as observed for spring. In agreement with the hot extremes  
52 indices, in general, the trends for the autumn are positive for the ERA-driven simulation and of  
53 opposite sign for the MPI-driven simulation, for the indices shown in this work.

54 For the winter months, the MPI-driven simulation showed a statistically significant increase in  
55 frost days and cold nights in the regions with higher altitude over the Iberian Peninsula.

56 For the ERA-driven simulation, the trends for the indices of cold extremes, are generally positive  
57 but these are not statistically significant and in some areas the trends are negative. In spite of the  
58 agreement between the results of the MPI and ERA driven simulations, this increase in the number  
59 of cold days and nights was not expected, and may be due to the fact that the hiatus period is  
60 included in the study period.  
61  
62  
63  
64  
65

1  
2  
3  
4  
5 - TNmean and TXmean time series:

6 When the trends are determined based on linear regression, it was observed that if the data have  
7 an irregular evolution in time this method would have few limitations. These limitations were  
8 identified in a paper by Tomé and Miranda (2004), where it is mentioned that this approach, although  
9 commonly used in variability studies, is not able to study the distribution of climate breakpoints in  
10 space and time.

11 The annual trend for the TN and TX simulations is higher for the ERA-driven simulation. A  
12 higher trend for TX in relation to TN was observed for both simulations (WRF forced by ERA and  
13 MPI). The seasonal trends of TN and TX for winter, both for ERA-driven and MPI-driven  
14 simulations, are negative. Several studies (Brunet et al., 2006; Brunet et al., 2007; El Kenawy et al.,  
15 2011; de Lima et al., 2013;) indicate a heating trend, so that negative trends for TX and TN, which  
16 point to a decrease in the winter temperature, were unexpected. These trends may be due to the fact  
17 that the warming hiatus is included in the period at study, leading to a negative trend. Furthermore,  
18 may also be a factor that the method used does not take into account the discontinuity points between  
19 trends with opposite signs.

20 For autumn, the trends in TN and TX for ERA-driven and MPI-driven simulations have a large  
21 difference. ERA has a negative trend, whereas MPI has a positive trend. The literature reports on the  
22 occurrence of the warming hiatus as a winter phenomenon, although it can start in autumn. For this  
23 reason, the biggest decrease in the TX variable, of  $-0.026^{\circ}\text{C}/\text{year}$ , is observed for autumn.

#### 24 **Acknowledgements:**

25 This study was supported by FEDER funds through the Programa Operacional Factores de  
26 Competitividade – COMPETE and by Portuguese national funds through FCT - Fundação para a  
27 Ciência e a Tecnologia, within the framework of the following projects: RESORT Project Reference  
28 PTDC/CTE-ATM/111508/2009; CLICURB EXCL/AAG-MAA/0383/2012.

#### 29 **REFERENCES**

- 30 Aguilar, E., Peterson, T. C., Obando, P. R., Frutos, R., Retana, J. A., Solera, M., et al., 2005.  
31 Changes in precipitation and temperature extremes in Central America and northern South  
32 America, 1961–2003. *Journal of Geophysical Research: Atmosphere* 110(D23), 1984–2012  
33 Alexander, L.V., Zhang, X., Peterson, T.C., Caesar, J., et al., 2006. Global observed changes in daily  
34 climate extremes of temperature and precipitation. *J. Geophys. Res.* 111, D05109.  
35 Barfus, K., Bernhofer, C., 2014. Assessment of GCM performances for the Arabian Peninsula,  
36 Brazil, and Ukraine and indications of regional climate change. *Environmental Earth  
37 Sciences*, 72(12), 4689-4703.  
38 Brands, S., Herrera, S., Fernández, J., Gutiérrez, J. M., 2013. How well do CMIP5 Earth System  
39 Models simulate present climate conditions in Europe and Africa?. *Climate dynamics*, 41(3-4),  
40 803-817.  
41 Brown, S. J., Caesar, J., Ferro, C. A., 2008. Global changes in extreme daily temperature since  
42 1950. *Journal of Geophysical Research: Atmospheres*. 113 (D5), 1984–2012.  
43 Brunet, M., Jones, P. D., Sigró, J., Saladié, O., Aguilar, E., Moberg, A., et al., 2007. Temporal and  
44 spatial temperature variability and change over Spain during 1850–2005. *Journal of Geophysical  
45 Research: Atmospheres* (1984–2012), 112(D12).  
46 Brunet, M., Saladié, O., Jones, P., Sigro, J., Aguilar, E., Moberg, A., et al., 2006. The development  
47 of a new dataset of Spanish daily adjusted temperature series (SDATS) (1850–  
48 2003). *International Journal of Climatology*, 26(13), 1777-1802.  
49  
50  
51  
52  
53  
54  
55  
56  
57  
58  
59  
60  
61  
62  
63  
64  
65

- 1  
2  
3  
4 Carvalho, D., Rocha, A., Gómez-Gesteira, M., Santos, C. S., 2014. Offshore wind energy resource  
5 simulation forced by different reanalyses: Comparison with observed data in the Iberian  
6 Peninsula. *Applied Energy*, 134, 57-64.
- 7 Ciais, P., Reichstein, M., Viovy, N., Granier, A., Ogée, J., Allard, V., et al., 2005. Europe-wide  
8 reduction in primary productivity caused by the heat and drought in 2003. *Nature*, 437(7058),  
9 529-533.
- 10 Cohen, J. L., Furtado, J. C., Barlow, M., Alexeev, V. A., Cherry, J. E., 2012. Asymmetric seasonal  
11 temperature trends. *Geophysical Research Letters*, 39(4).
- 12 Cruz, R., Lage, A., 2006. Análisis de la evolución de la temperatura y precipitación en el periodo  
13 1973–2004 en Galicia. In *Clima, Sociedad y Medio Ambiente. V Congreso de la AEC.*  
14 *Asociación Española de Climatología, Zaragoza (Vol. 113).*
- 15 Dasari, H. P., Pozo, I., Ferri-Yáñez, F., Araújo, M. B., 2014. A Regional Climate Study of Heat  
16 Waves over the Iberian Peninsula. *Atmospheric and Climate Sciences*, 4(05), 841.
- 17 de Lima, M. I. P., Santo, F. E., Ramos, A. M., , de Lima, J. L., 2013. Recent changes in daily  
18 precipitation and surface air temperature extremes in mainland Portugal, in the period 1941–  
19 2007. *Atmospheric Research*, 127, 195-209.
- 20 Dee, D. P., Uppala, S. M., Simmons, A. J., Berrisford, P., Poli, P., Kobayashi, S., et al., 2011. The  
21 ERA-Interim reanalysis: Configuration and performance of the data assimilation  
22 system. *Quarterly Journal of the Royal Meteorological Society*, 137(656), 553-597.
- 23 Del Rio, S., Fraile, R., Herrero, L., Penas, A., 2007. Analysis of recent trends in mean maximum and  
24 minimum temperatures in a region of the NW of Spain (Castilla y León). *Theoretical and  
25 applied Climatology*, 90(1-2), 1-12.
- 26 Del Río, S., Herrero, L., Pinto-Gomes, C., Penas, A., 2011. Spatial analysis of mean temperature  
27 trends in Spain over the period 1961–2006. *Global and Planetary Change*, 78(1), 65-75.
- 28 Easterling, D. R., Wehner, M. F., 2009. Is the climate warming or cooling?. *Geophysical Research  
29 Letters*, 36(8).
- 30 Efthymiadis, D., Goodess, C. M., Jones, P. D., 2011. Trends in Mediterranean gridded temperature  
31 extremes and large-scale circulation influences. *Natural Hazards and Earth System  
32 Science*, 11(8), 2199-2214.
- 33 El Kenawy, A. M., López-Moreno, J. I., Vicente Serrano, S. M., 2011. Recent trends in daily  
34 temperature extremes over northeastern Spain (1960–2006). *Natural Hazards and Earth System  
35 Sciences*, 11(9), 2583-2603.
- 36 England, M. H., McGregor, S., Spence, P., Meehl, G. A., Timmermann, A., Cai, W., et al., 2014.  
37 Recent intensification of wind-driven circulation in the Pacific and the ongoing warming  
38 hiatus. *Nature Climate change*, 4(3), 222-227.
- 39 Espírito Santo, F., de Lima, I. P., Silva, Á., Pires, V., de Lima, J. L., 2014. Spatio-temporal  
40 variability of dry and wet periods in mainland Portugal and its relationships with teleconnection  
41 patterns. In *EGU General Assembly Conference Abstracts (Vol. 16, p. 16446).*
- 42 Esteban-Parra, M. J., Rodrigo, F. S., Castro-Díez, Y., 1995. Temperature trends and change points in  
43 the Northern Spanish Plateau during the last 100 years. *International Journal of  
44 Climatology*, 15(9), 1031-1042.
- 45 Fernández-Montes, S., Rodrigo, F. S., 2012. Trends in seasonal indices of daily temperature  
46 extremes in the Iberian Peninsula, 1929–2005. *International Journal of Climatology*, 32(15),  
47 2320-2332.
- 48 Field, C. B. (Ed.), 2012. *Managing the risks of extreme events and disasters to advance climate  
49 change adaptation: special report of the intergovernmental panel on climate change.* Cambridge  
50 University Press.
- 51 Fyfe, J. C., Gillett, N. P., Zwiers, F. W., 2013. Overestimated global warming over the past 20  
52 years. *Nature Climate Change*, 3(9), 767-769.
- 53  
54  
55  
56  
57  
58  
59  
60  
61  
62  
63  
64  
65

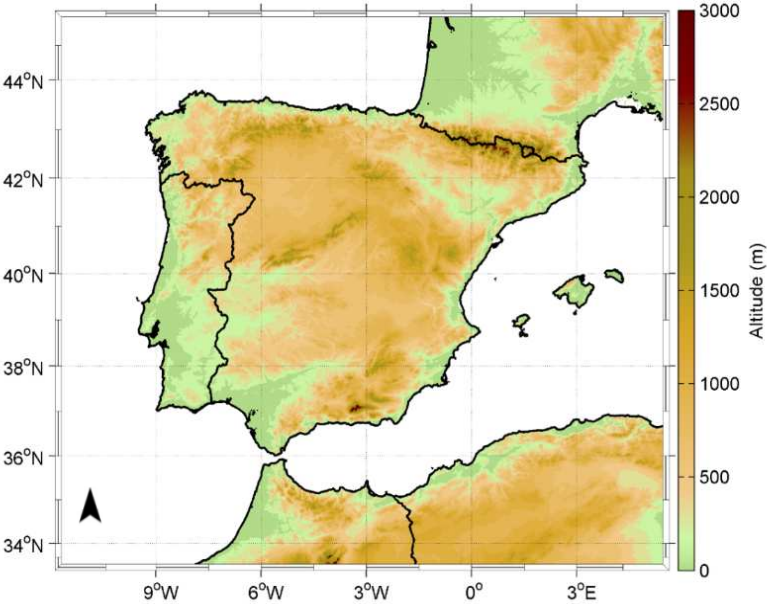
- 1  
2  
3  
4 García-Herrera, R., Díaz, J., Trigo, R. M., Hernández, E., 2005. Extreme summer temperatures in  
5 Iberia: health impacts and associated synoptic conditions. In *Annales Geophysicae* (Vol. 23, No.  
6 2, pp. 239-251).
- 7 Griffiths, G. M., Chambers, L. E., Haylock, M. R., Manton, M. J., Nicholls, N., Baek, H. J., et al.,  
8 2005. Change in mean temperature as a predictor of extreme temperature change in the Asia-  
9 Pacific region. *International Journal of Climatology*, 25(10), 1301-1330.
- 10 Karl, T. R., Knight, R. W., Gallo, K. P., Peterson, T. C., Jones, P. D., Kukla, G., et al., 1993. A new  
11 perspective on recent global warming: asymmetric trends of daily maximum and minimum  
12 temperature. *Bulletin of the American Meteorological Society*, 74(6), 1007-1023.
- 13 Karl, T. R., Nicholls, N., Ghazi, A., 1999. Clivar/GCOS/WMO workshop on indices and indicators  
14 for climate extremes workshop summary. In *Weather and Climate Extremes* (pp. 3-7). Springer  
15 Netherlands.
- 16 Kaufmann, R. K., Kauppi, H., Mann, M. L., Stock, J. H., 2011. Reconciling anthropogenic climate  
17 change with observed temperature 1998–2008. *Proceedings of the National Academy of  
18 Sciences*, 108(29), 11790-11793.
- 19 Kharin, V. V., Zwiers, F. W., 2000. Changes in the extremes in an ensemble of transient climate  
20 simulations with a coupled atmosphere-ocean GCM. *Journal of Climate*, 13(21), 3760-3788.
- 21 Klein Tank, A. M. G., Können, G. P., 2003. Trends in indices of daily temperature and precipitation  
22 extremes in Europe, 1946-99. *Journal of Climate*, 16(22), 3665-3680.
- 23 Klein Tank, A. M. G., Wijngaard, J. B., Können, G. P., Böhm, R., Demarée, G., Gocheva, A., et al.  
24 2002. Daily dataset of 20th-century surface air temperature and precipitation series for the  
25 European Climate Assessment. *International Journal of Climatology*, 22(12), 1441-1453.
- 26 Kosaka, Y., Xie, S. P., 2013. Recent global-warming hiatus tied to equatorial Pacific surface  
27 cooling. *Nature*, 501(7467), 403-407.
- 28 Kuglitsch, F. G., Toreti, A., Xoplaki, E., Della-Marta, P. M., Zerefos, C. S., Türkeş, M., Luterbacher,  
29 J., 2010. Heat wave changes in the eastern Mediterranean since 1960. *Geophysical Research  
30 Letters*, 37(4).
- 31 Manton, M. J., Della-Marta, P. M., Haylock, M. R., Hennessy, K. J., Nicholls, N., Chambers, L. E.,  
32 et al. 2001. Trends in extreme daily rainfall and temperature in Southeast Asia and the South  
33 Pacific: 1961–1998. *International Journal of Climatology*, 21(3), 269-284 (Current issue)
- 34 Marta-Almeida, Teixeira, J., Carvalho, M. J., Melo-Gonçalves, P. M., Rocha, 2015. High resolution  
35 climatic simulations for the Iberian Peninsula: Model validation. *Physics and Chemistry of the  
36 Earth*, 2015. (current issue)
- 37 Martínez, M. D., Serra, C., Burgueño, A., Lana, X., 2010. Time trends of daily maximum and  
38 minimum temperatures in Catalonia (ne Spain) for the period 1975–2004. *International Journal  
39 of Climatology*, 30(2), 267-290.
- 40 Meehl, G. A., Arblaster, J. M., Fasullo, J. T., Hu, A., Trenberth, K. E., 2011. Model-based evidence  
41 of deep-ocean heat uptake during surface-temperature hiatus periods. *Nature Climate  
42 Change*, 1(7), 360-364.
- 43 Moberg, A., Jones, P. D., 2005. Trends in indices for extremes in daily temperature and precipitation  
44 in central and western Europe, 1901–99. *International Journal of Climatology*, 25(9), 1149-1171.
- 45 Moberg, A., Jones, P. D., Lister, D., Walther, A., Brunet, M., Jacobeit, J., et al., 2006. Indices for  
46 daily temperature and precipitation extremes in Europe analyzed for the period 1901–  
47 2000. *Journal of Geophysical Research: Atmospheres* (1984–2012), 111(D22).
- 48 Moss, R. H., Edmonds, J. A., Hibbard, K. A., Manning, M. R., Rose, S. K., Van Vuuren, D. P., et al.,  
49 2010. The next generation of scenarios for climate change research and  
50 assessment. *Nature*, 463(7282), 747-756.
- 51  
52  
53  
54  
55  
56  
57  
58  
59  
60  
61  
62  
63  
64  
65

- 1  
2  
3  
4 New, M., Hewitson, B., Stephenson, D. B., Tsiga, A., Kruger, A., Manhique, A., et al., 2006.  
5 Evidence of trends in daily climate extremes over southern and west Africa. *Journal of*  
6 *Geophysical Research: Atmospheres* (1984–2012), 111(D14).  
7 Patz, J. A., Campbell-Lendrum, D., Holloway, T., Foley, J. A., 2005. Impact of regional climate  
8 change on human health. *Nature*, 438(7066), 310-317.  
9 Peterson, T. C., Taylor, M. A., Demeritte, R., Duncombe, D. L., Burton, S., Thompson, F., et al.,  
10 2002. Recent changes in climate extremes in the Caribbean region. *Journal of Geophysical*  
11 *Research: Atmospheres* (1984–2012), 107(D21), ACL-16.  
12 Peterson, T., Folland, C., Gruza, G., Hogg, W., Mokssit, A., Plummer, N., 2001. Report on the  
13 activities of the working group on climate change detection and related rapporteurs. Geneva:  
14 World Meteorological Organization.  
15 Prieto, L., Herrera, R. G., Díaz, J., Hernández, E., del Teso, T., 2004. Minimum extreme  
16 temperatures over Peninsular Spain. *Global and Planetary Change*, 44(1), 59-71.  
17 Rodríguez-Puebla, C., Encinas, A. H., García-Casado, L. A., Nieto, S., 2010. Trends in warm days  
18 and cold nights over the Iberian Peninsula: relationships to large-scale variables. *Climatic*  
19 *Change*, 100(3-4), 667-684.  
20 Schliep, E. M., Cooley, D., Sain, S. R., Hoeting, J. A., 2010. A comparison study of extreme  
21 precipitation from six different regional climate models via spatial hierarchical  
22 modeling. *Extremes*, 13(2), 219-239.  
23 Sen, P. K., 1968. Estimates of the regression coefficient based on Kendall's tau. *Journal of the*  
24 *American Statistical Association*, 63(324), 1379-1389.  
25 Seneviratne, S. I., Donat, M. G., Mueller, B., Alexander, L. V., 2014. No pause in the increase of hot  
26 temperature extremes. *Nature Climate Change*, 4(3), 161-163.  
27 Sillmann, J., Donat, M. G., Fyfe, J. C., Zwiers, F. W., 2014. Observed and simulated temperature  
28 extremes during the recent warming hiatus. *Environmental Research Letters*, 9(6), 064023.  
29 Sillmann, J., Kharin, V. V., Zhang, X., Zwiers, F. W., Bronaugh, D., 2013a. Climate extremes  
30 indices in the CMIP5 multimodel ensemble: Part 1. Model evaluation in the present  
31 climate. *Journal of Geophysical Research: Atmospheres*, 118(4), 1716-1733.  
32 Sillmann, J., Kharin, V. V., Zwiers, F. W., Zhang, X., Bronaugh, D., 2013b. Climate extremes  
33 indices in the CMIP5 multimodel ensemble: Part 2. Future climate projections. *Journal of*  
34 *Geophysical Research: Atmospheres*, 118(6), 2473-2493.  
35 Simolo, C., Brunetti, M., Maugeri, M., Nanni, T., 2011. Evolution of extreme temperatures in a  
36 warming climate. *Geophysical Research Letters*, 38(16).  
37 Skamarock, W. C., Klemp, J. B., Dudhia, J., Gill, D. O., Barker, D. M., Duda, M. G., et al., 2008.  
38 NCAR Technical Note: A Description of the Advanced Research WRF Version 3; Mesoscale ,  
39 Microscale Meteorology Division. National Center for Atmospheric Research, Boulder, CO,  
40 USA.  
41 Solomon, S., Daniel, J. S., Neely, R. R., Vernier, J. P., Dutton, E. G., Thomason, L. W., 2011. The  
42 persistently variable “background” stratospheric aerosol layer and global climate  
43 change. *Science*, 333(6044), 866-870.  
44 Solomon, S., Rosenlof, K. H., Portmann, R. W., Daniel, J. S., Davis, S. M., Sanford, T. J., Plattner,  
45 G. K., 2010. Contributions of stratospheric water vapor to decadal changes in the rate of global  
46 warming. *Science*, 327(5970), 1219-1223.  
47 Taylor, K. E., Stouffer, R. J., Meehl, G. A., 2012. An overview of CMIP5 and the experiment  
48 design. *Bulletin of the American Meteorological Society*, 93(4), 485-498.  
49 Theil, H. (1950). A rank-invariant method of linear and polynomial regression analysis, I. *Proc. Kon.*  
50 *Ned. Akad. v. Wetensch.* A53, 386-392.  
51 Tomé, A. R., Miranda, P. M. A., 2004. Piecewise linear fitting and trend changing points of climate  
52 parameters. *Geophysical Research Letters*, 31(2).  
53  
54  
55  
56  
57  
58  
59  
60  
61  
62  
63  
64  
65

1  
2  
3  
4  
5  
6  
7  
8  
9  
10  
11  
12  
13  
14  
15  
16  
17  
18  
19  
20  
21  
22  
23  
24  
25  
26  
27  
28  
29  
30  
31  
32  
33  
34  
35  
36  
37  
38  
39  
40  
41  
42  
43  
44  
45  
46  
47  
48  
49  
50  
51  
52  
53  
54  
55  
56  
57  
58  
59  
60  
61  
62  
63  
64  
65

Wilks, D. S., 2011. Statistical methods in the atmospheric sciences (Vol. 100). Academic press.  
Zhang, X., Alexander, L., Hegerl, G. C., Jones, P., Tank, A. K., Peterson, T. C., et al., 2011. Indices for monitoring changes in extremes based on daily temperature and precipitation data. Wiley Interdisciplinary Reviews: Climate Change, 2(6), 851-870.

1  
2  
3  
4 **List of the figures**  
5  
6  
7  
8



28 **Fig. 1. Location of the study area and the simulation domain (<http://www.ngdc.noaa.gov/mgg/global/global.html>)**  
29  
30  
31  
32  
33  
34  
35  
36  
37  
38  
39  
40  
41  
42  
43  
44  
45  
46  
47  
48  
49  
50  
51  
52  
53  
54  
55  
56  
57  
58  
59  
60  
61  
62  
63  
64  
65

1  
2  
3  
4  
5  
6  
7  
8  
9  
10  
11  
12  
13  
14  
15  
16  
17  
18  
19  
20  
21  
22  
23  
24  
25  
26  
27  
28  
29  
30  
31  
32  
33  
34  
35  
36  
37  
38  
39  
40  
41  
42  
43  
44  
45  
46  
47  
48  
49  
50  
51  
52  
53  
54  
55  
56  
57  
58  
59  
60  
61  
62  
63  
64  
65

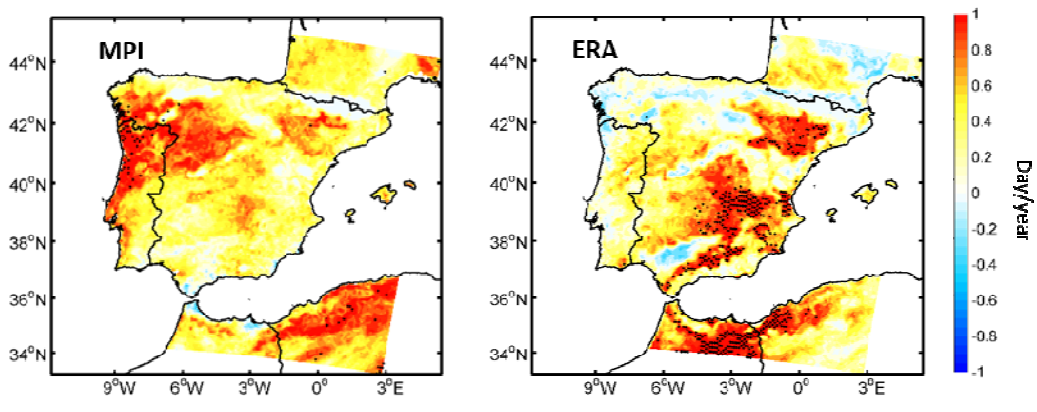


**Fig 2. Annual trends of SU (summer days) for the period of 1986-2005 over Iberian Peninsula for WRF forced by MPI (left) and ERA (right). Dots represent grid points where the trend is statistically significant at a 0.05 significance level**

1  
2  
3  
4  
5  
6  
7  
8  
9  
10  
11  
12  
13  
14  
15  
16  
17  
18  
19  
20  
21  
22  
23  
24  
25  
26  
27  
28  
29  
30  
31  
32  
33  
34  
35  
36  
37  
38  
39  
40  
41  
42  
43  
44  
45  
46  
47  
48  
49  
50  
51  
52  
53  
54  
55  
56  
57  
58  
59  
60  
61  
62  
63  
64  
65

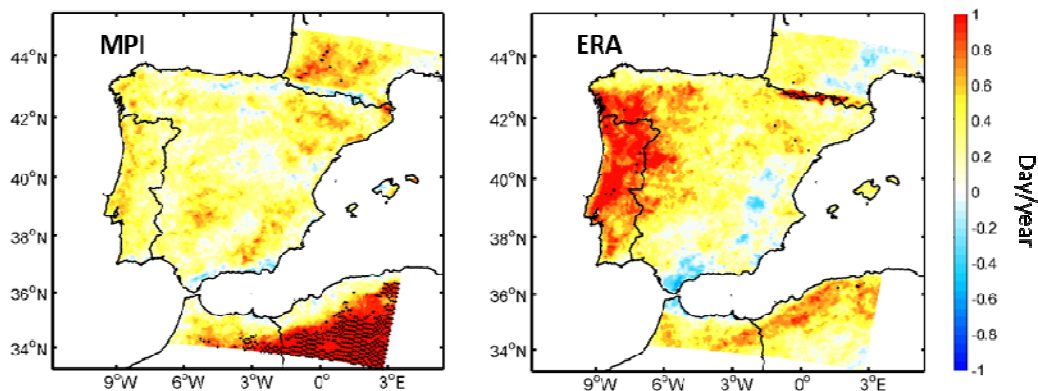


**Fig 3.** Annual trends of TX90p (Warm days) for the period of 1986-2005 over Iberian Peninsula for WRF forced by MPI (left) and ERA (right). Dots represent grid points where the trend is statistically significant at a 0.05 significance level

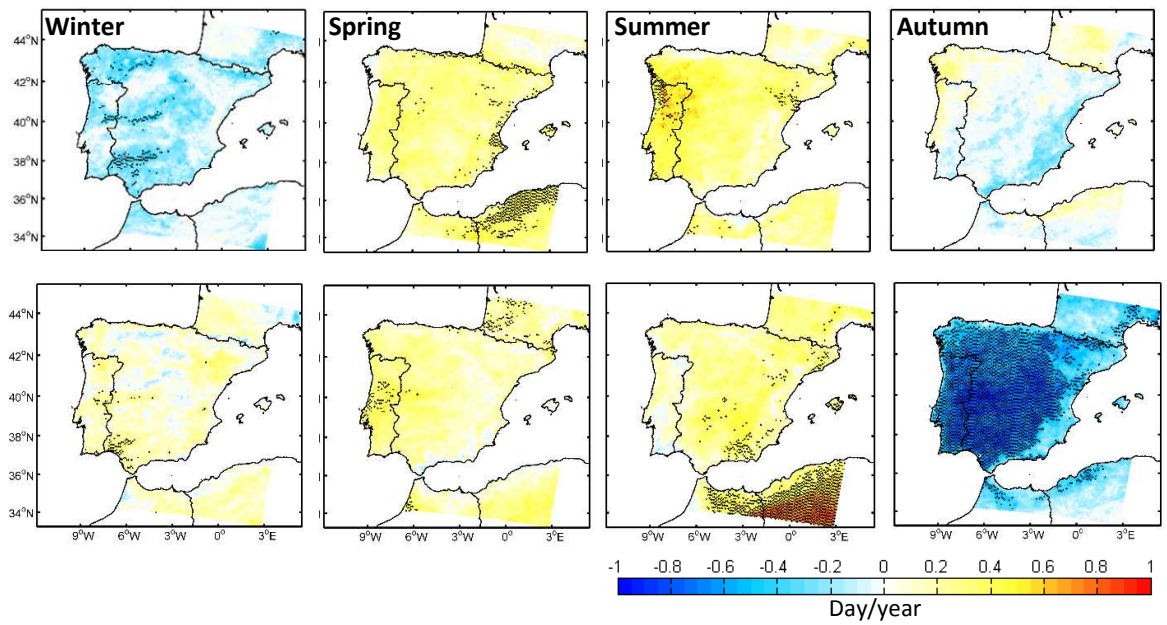


**Fig. 4.** Seasonal trends of TX90p (Warm Days) for the period of 1986-2005 over Iberian Peninsula for WRF forced by MPI (top) and ERA (down). Dots represent grid points where the trend is statistically significant at a 0.05 significance level

1  
2  
3  
4  
5  
6  
7  
8  
9  
10  
11  
12  
13  
14  
15  
16  
17  
18  
19  
20  
21  
22  
23  
24  
25  
26  
27  
28  
29  
30  
31  
32  
33  
34  
35  
36  
37  
38  
39  
40  
41  
42  
43  
44  
45  
46  
47  
48  
49  
50  
51  
52  
53  
54  
55  
56  
57  
58  
59  
60  
61  
62  
63  
64  
65

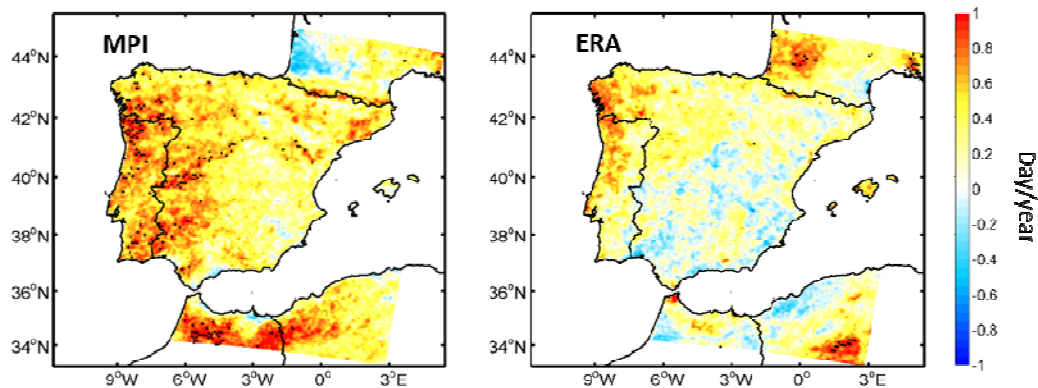


Fig. 5. Annual trends of TN90p (Warm nights) for the period of 1986-2005 over Iberian Peninsula for WRF forced by MPI (left) and ERA (right). Dots represent grid points where the trend is statistically significant at a 0.05 significance level

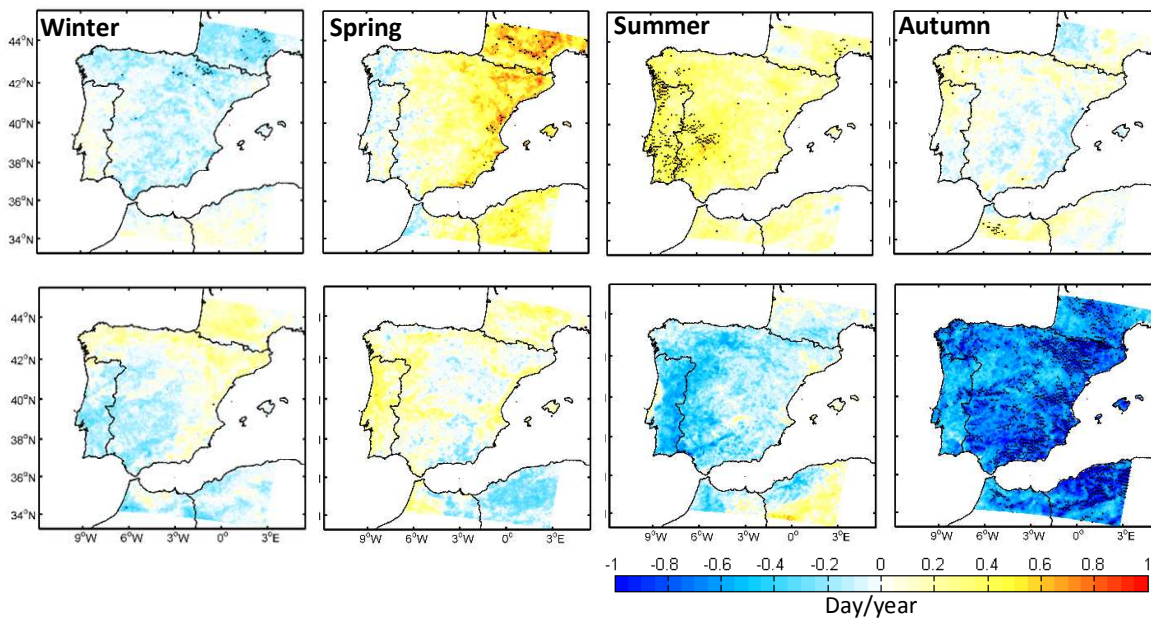
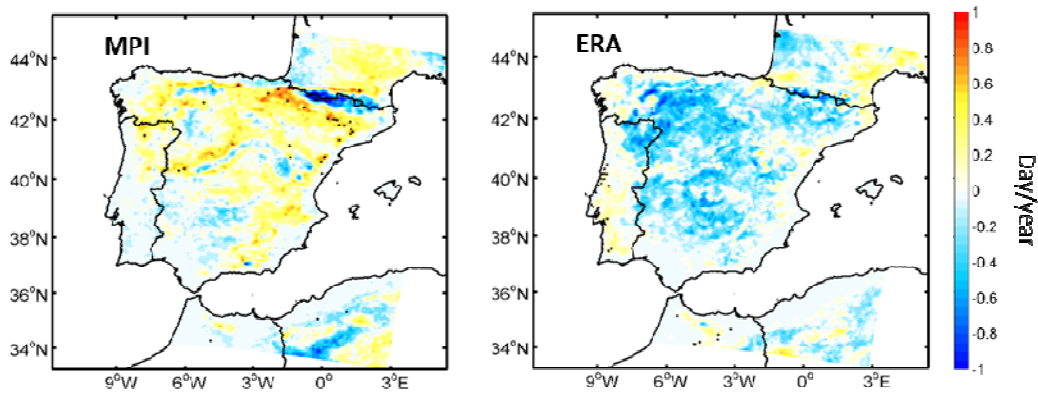


Fig. 6. Seasonal trends of TN90p (Warm Nights) for the period of 1986-2005 over Iberian Peninsula for WRF forced by MPI (top) and ERA (down). Dots represent grid points where the trend is statistically significant at a 0.05 significance level

1  
2  
3  
4  
5  
6  
7  
8  
9  
10  
11  
12  
13  
14  
15  
16  
17  
18  
19  
20  
21  
22  
23  
24  
25  
26  
27  
28  
29  
30  
31  
32  
33  
34  
35  
36  
37  
38  
39  
40  
41  
42  
43  
44  
45  
46  
47  
48  
49  
50  
51  
52  
53  
54  
55  
56  
57  
58  
59  
60  
61  
62  
63  
64  
65



**Fig 7. Annual trends of FD (frost days) for the period of 1986-2005 over Iberian Peninsula for WRF forced by MPI (left) and ERA (right). Dots represent grid points where the trend is statistically significant at a 0.05 significance level**

1  
2  
3  
4  
5  
6  
7  
8  
9  
10  
11  
12  
13  
14  
15  
16  
17  
18  
19  
20  
21  
22  
23  
24  
25  
26  
27  
28  
29  
30  
31  
32  
33  
34  
35  
36  
37  
38  
39  
40  
41  
42  
43  
44  
45  
46  
47  
48  
49  
50  
51  
52  
53  
54  
55  
56  
57  
58  
59  
60  
61  
62  
63  
64  
65

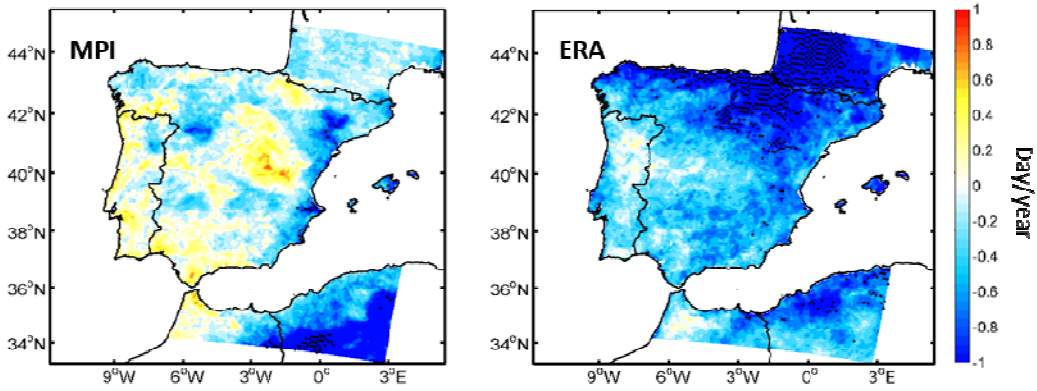


Fig 8. Annual trends of TX10p (cold days) for the period of 1986-2005 over Iberian Peninsula for WRF forced by MPI (left) and ERA (right). Dots represent grid points where the trend is statistically significant at a 0.05 significance level

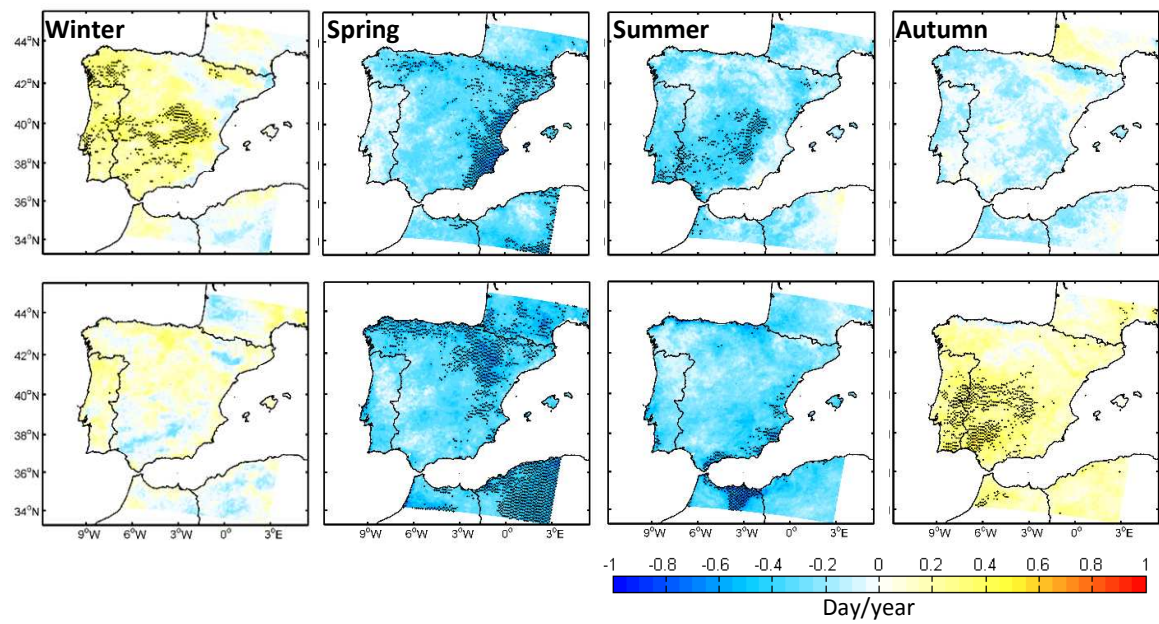


Fig. 9. Seasonal trends of TX10p (cold days) for the period of 1986-2005 over Iberian Peninsula for WRF forced by MPI (top) and ERA (down). Dots represent grid points where the trend is statistically significant at a 0.05 significance level

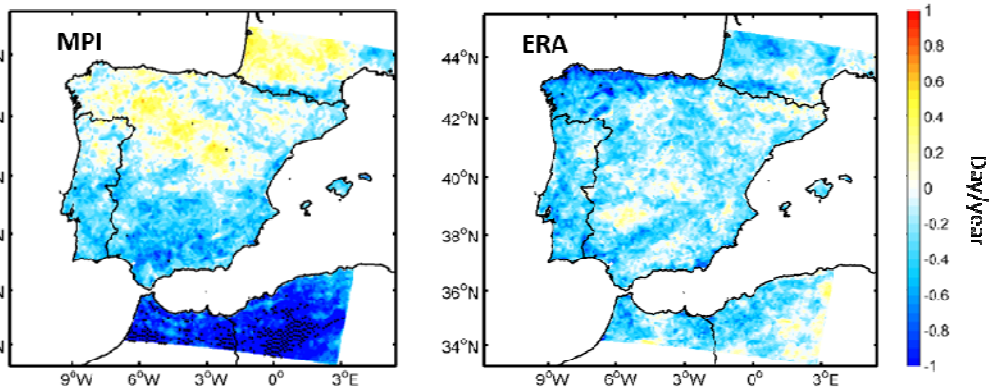


Fig 10. Annual trends of TN10p (Cold nights) for the period of 1986-2005 over Iberian Peninsula for WRF forced by MPI (left) and ERA (right). Dots represent grid points where the trend is statistically significant at a 0.05 significance level

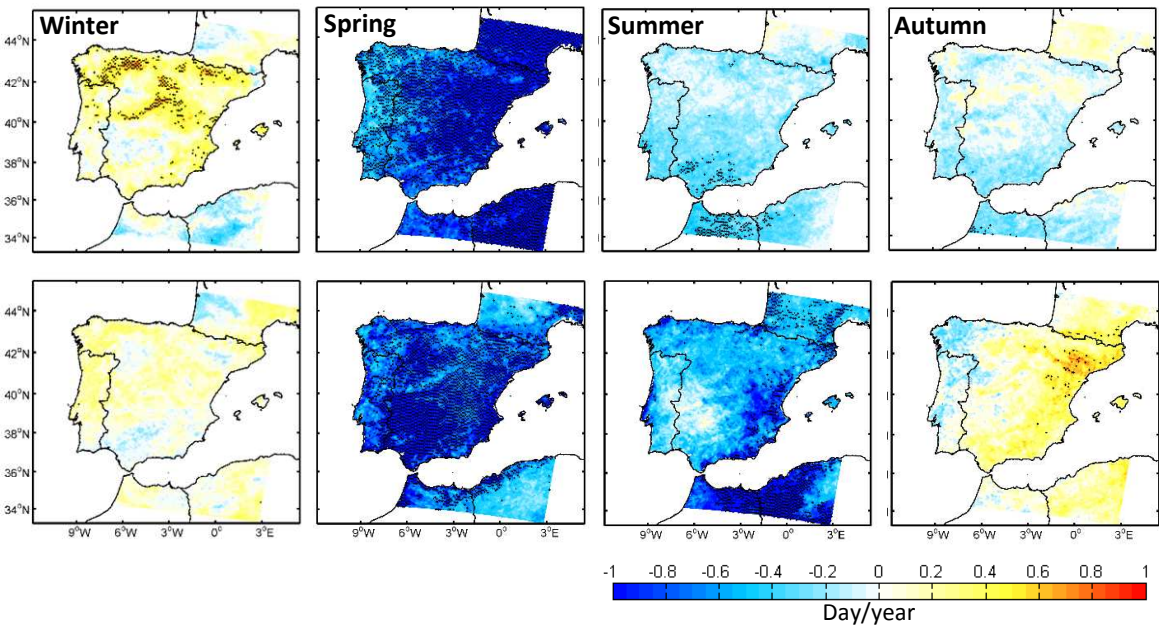


Fig. 11. Seasonal trends of TN10p (Cold Nights) for the period of 1986-2005 over Iberian Peninsula for WRF forced by MPI (top) and ERA (down). Dots represent grid points where the trend is statistically significant at a 0.05 significance level

1  
2  
3  
4  
5  
6  
7  
8  
9  
10  
11  
12  
13  
14  
15  
16  
17  
18  
19  
20  
21  
22  
23  
24  
25  
26  
27  
28  
29  
30  
31  
32  
33  
34  
35  
36  
37  
38  
39  
40  
41  
42  
43  
44  
45  
46  
47  
48  
49  
50  
51  
52  
53  
54  
55  
56  
57  
58  
59  
60  
61  
62  
63  
64  
65

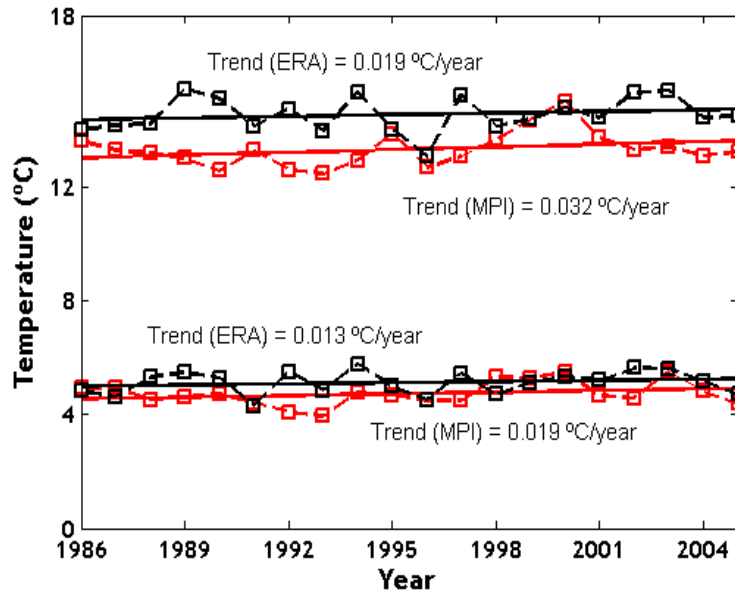


Fig. 12. Annual spatial means (dashed lines) of maximum temperature (above) and minimum temperature (below) for the WRF simulations forced by MPI (black) and ERA-Interim (red) with corresponding trend lines

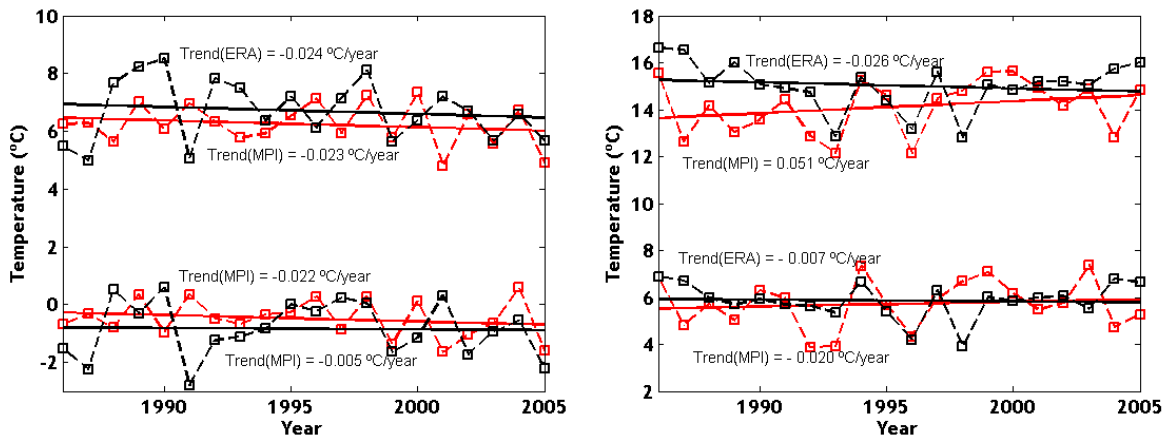


Fig. 3. Spatial average for winter (a) and autumn (b) of maximum temperature (above) and minimum temperature (below) for the WRF simulations forced by MPI (black) and ERA-Interim (red) with corresponding trend lines

1  
2  
3  
4  
5  
6  
7  
8  
9  
10  
11  
12  
13  
14  
15  
16  
17  
18  
19  
20  
21  
22  
23  
24  
25  
26  
27  
28  
29  
30  
31  
32  
33  
34  
35  
36  
37  
38  
39  
40  
41  
42  
43  
44  
45  
46  
47  
48  
49  
50  
51  
52  
53  
54  
55  
56  
57  
58  
59  
60  
61  
62  
63  
64  
65

**Table 1. List of all extreme temperatures indices. The present study concentrated on those indices that are underlined**

<b>ID</b>	<b>Name</b>	<b>Definitions</b>	<b>Units</b>	
<u>SU</u>	Summer days	Annual count when TX > 25 °C	days	<b>Hot Extremes</b>
TR	Tropical nights	Annual count when TN >20 °C	days	
TXx	Max TX	Maximum value of daily TX	°C	
TXn	Min TX	Minimum value of daily TX	°C	
<u>TN90p</u>	Warm nights	Percentage of days when TN>90th percentile of 1986–2005	days	
<u>TX90p</u>	Warm days	Percentage of days when TX>90th percentile of 1986–2005	days	
CSDI	Cold spell duration index	Annual count of days with at least 6 consecutive days when TN < 10th percentile	days	<b>Cold Extremes</b>
<u>FD</u>	Frost days	Annual count when TN < 0 °C	days	
ID	Ice days	Annual count when TX <0 °C	days	
TNx	Max TN	Maximum value of daily TN	°C	
TNn	Min TN	Minimum value of daily TN	°C	
<u>TN10p</u>	Cool nights	Percentage of days when TN<10th percentile of 1986–2005	days	
<u>TX10p</u>	Cool days	Percentage of days when TX<10th percentile of 1986–2005	days	<b>Variability extremes</b>
WSDI	Warm spell duration index	Annual count of days with at least 6 consecutive days when TX > 90th percentile	days	
DTR	Diurnal temperature range	Yearly mean difference between TX and TN	°C	
ETR	Extreme temperature range	Difference between TXx and TNn	°C	
GSL	Growing season length	Annual count of days between the first span of at least 6 days with $T_{\text{mean}} > 5^{\circ}\text{C}$ and first span after 1 July of 6 days with $T_{\text{mean}} < 5^{\circ}\text{C}$	days	